Proceedings of 2011 International Microwave Symposium, Baltimore, MD, June 2011.

Integrated Antenna/Electro-Optic Modulator for RF Photonic Front-Ends

Rodney B. Waterhouse and Dalma Novak

Pharad, LLC, Glen Burnie, MD, 21061, USA

***Abstract* — We present an efficient, integrated antenna/electro-optic modulator assembly for RF photonic front-ends in phased array applications. The integrated radiator/photonic device incorporates a non-contact fed stacked patch antenna that has been designed to radiate efficiently between 9 – 11 GHz and is easily coupled to the Lithium Niobate Mach-Zehnder modulator, requiring minimal modification to the electrode structure of this photonic device. We discuss the design procedure for the integrated assembly, the predicted characteristics of the antenna in this environment and test a proof-of-concept version of the module. Finally we verify the performance of the module through a link demonstration.**

***Index Terms* — Microwave photonics, integrated antennas, optical modulators, phased arrays, printed antennas.**

I. Introduction

The application of RF photonic links for fiber remoting of phased array antennas and wireless communication systems continues to evolve with recent developments in RF photonic device technologies, transmission techniques and receiver architectures [1]. A fundamental aspect of the implementation of next generation high performance communication systems is the creation of efficient wideband transducers from free-space RF to the guided optical domain and vice-versa. It is imperative that the insertion loss of these interfaces is kept to a minimum, as this will directly impact the dynamic range of the system and therefore the overall capacity.

Figure 1 illustrates the general architecture of a fiber remoted phased array antenna that incorporates a photonic-based RF front-end. Here the radar waveform to be transmitted by each individual element in the antenna array is generated remotely from the antenna and the full RF signal is encoded onto an optical source (E/O conversion) for transport over fiber to the remote antenna. The optical signal is then detected at each antenna array element by a photodetector (PD) to regenerate the encoded transmit waveform.

As depicted in Figure 1, in a fiber remoted phased array system the detected transmit waveform is amplified in a high power amplifier (HPA), for example, which then directly drives the antenna element. For the receiver portion of the phased array radar RF front-end, the return signal is captured by a receive antenna element (which may be the same as the transmit antenna), amplified in a low noise amplifier (LNA), and then encoded onto the amplitude or phase of an optical carrier using an electro-optic modulator (EOM) for transport over fiber back to a central location where appropriate electronics digitize and process the signal.

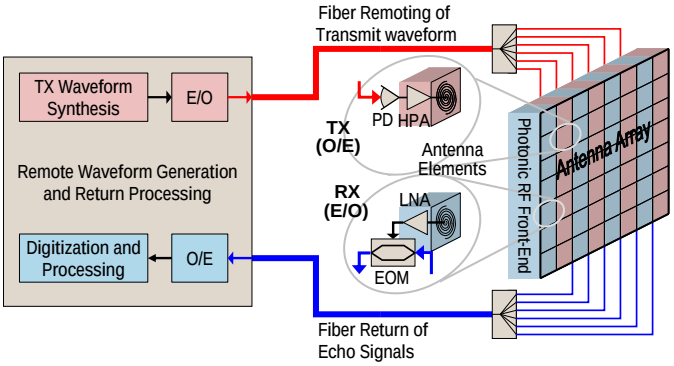

Fig. 1. Schematic showing the architecture of a fiber remoted radar system and electro-optic RF front-end.

The generic radar architecture shown in Figure 1 includes amplifiers between the photonic components and the antenna elements, however increasing the overall efficiency of the RF photonic link may remove the need for any electronic amplification at the Transmit (TX) and (Receive) RX antenna. This could be achieved through devices that improve the E/O (electrical to optical) and O/E (optical to electrical) conversion processes, as well as techniques to increase the power transferred between the antenna and the photodetector or electro-optic modulator. A significant challenge in increasing RF photonic link efficiency is how to increase the transfer of power between the RF and optical domains over a wide operating bandwidth.

In this paper, we present the design and experimental verification of a novel, efficient integrated antenna/modulator assembly. The integrated module was designed for efficient operation over the frequency range of 9 – 11 GHz. The assembly utilizes a proximity coupled stacked patch antenna that is placed over the Lithium Niobate ($LiNbO_3$) wafer of the EOM and requires minimal modification to the electrodes of the wafer itself. We utilized a full-wave electromagnetic simulation tool (CST™) to accurately model the performance of the antenna when coupled to the $LiNbO_3$ wafer and located in the modified housing for the electro-optic modulator. We then made modifications to the antenna to ensure it would operate efficiently in this environment. We created a proof-of-concept version of the antenna to verify its electromagnetic (EM) performance and then developed the integrated antenna/EOM module. We undertook an experimental link investigation of the proposed integrated antenna/EOM assembly and demonstrated its efficient operation over 9 – 11 GHz.

Proceedings of 2011 International Microwave Symposium, Baltimore, MD, June 2011.

II. Configuration And Design Procedure

Figure 2 shows a schematic of the proposed integrated module showing the printed antenna within the casing of a conventional high-speed electro-optic modulator and coupled to the electrode structure of the photonic device. To simplify the design procedure for the integrated antenna/modulator assembly and also to reduce the cost of the resulting module, we utilized a non-contact feed printed antenna to couple free-space RF energy to the electro-optic modulator. Doing so meant that we did not have to modify the electrode structure of a conventional $LiNbO_3$ modulator. The antenna could simply be positioned above the electrodes (using support material to ensure the electrodes of the modulator are not damaged) and adhered to the casing of the photonic component.

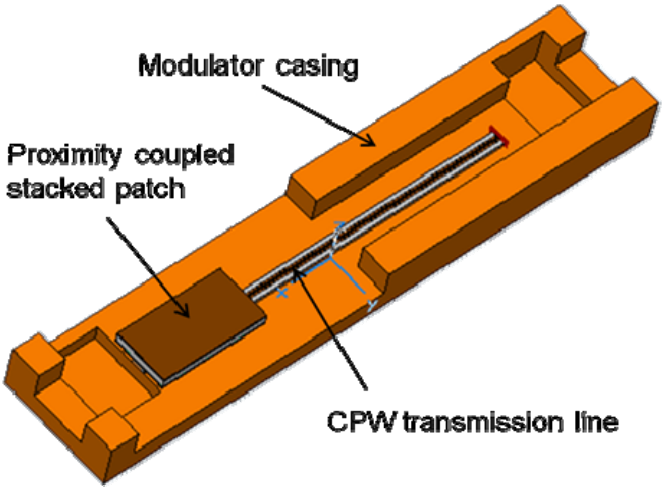

Fig. 2. Schematic of integrated antenna/EOM module (without cover).

As can be seen in Figure 2, the lid of the electro-optic modulator package has been removed (this original metallic lid was later replaced with a Rexolite structure). Also, part of the side walls of the modulator casing have been removed to ensure the antenna is not shorted at these locations. These gaps in the package walls were also replaced with Rexolite sections.

The antenna to be directly integrated with the electro-optic modulator consists of multiple dielectric layers and two vertically coupled patches. Figure 3 shows a cross-sectional view of the printed antenna. Here two support layers of Arlon 450 are used to ensure the electrodes of the modulator are not damaged and a superstrate layer is incorporated to protect the antenna. The ground-plane for the antenna is the casing of the modulator.

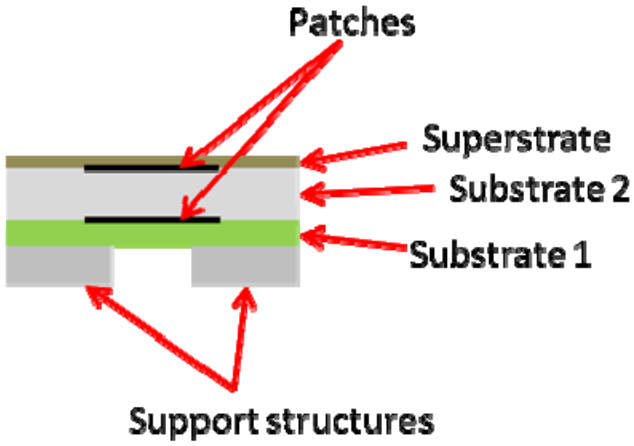

Fig. 3. Cross-sectional view of proposed printed antenna.

The design procedure for the integrated antenna typically involves seven steps. Firstly, we design a simple proximity coupled stacked patch to operate over the appropriate frequency range (here 9 – 11 GHz) using the procedure highlighted in [2], assuming dielectric layers and a ground-plane that have infinite extent in the horizontal directions. We also use a 'surrogate' high dielectric constant feed material (typically Rogers RT/Duroid 6010) due to the uniaxial anisotropic properties of $LiNbO_3$. In this initial design step we also use a microstrip feed, as opposed to a coplanar waveguide feed (CPW); once again due to its simplicity. Once a good match over the designed frequency band is achieved for the integrated antenna, we progressively modify the structure until it looks like the resulting configuration shown in Figure 2. In each stage, we modify the dimensions of the patches and the heights of the dielectric laminates to ensure good interactions between the patches occur and therefore good matching is evident over the appropriate frequency band.

In the second stage of the design phase of the integrated antenna, we truncate the feed substrate to be consistent with the dimensions of the EOM wafer and also truncate the other dielectric laminates. The next step is to replace the microstrip feed with a CPW feed. The following two stages involve truncating the size of the ground-plane and also replacing the surrogate feed material with $LiNbO_3$. The final two stages involve modeling the integrated antenna in the EOM casing (as shown in Figure 2) and then with the Rexolite cover and side wall sections. It is interesting to note that the dimensions of the antenna do not really change much through this design process from that established in the first step. Probably the biggest modification occurs in the second stage where the feed material is truncated. Here, the dimensions of the lower patch are increased because since we truncate the feed substrate, the lower patch 'sees' less of the high dielectric constant material.

Figure 4 shows the predicted reflection coefficient of the proposed integrated antenna and as can be seen from this plot, the antennas displays a good impedance match over 9 – 11 GHz. The -10 dB reflection coefficient bandwidth of approximately 20 % is consistent with this form of radiator [2].

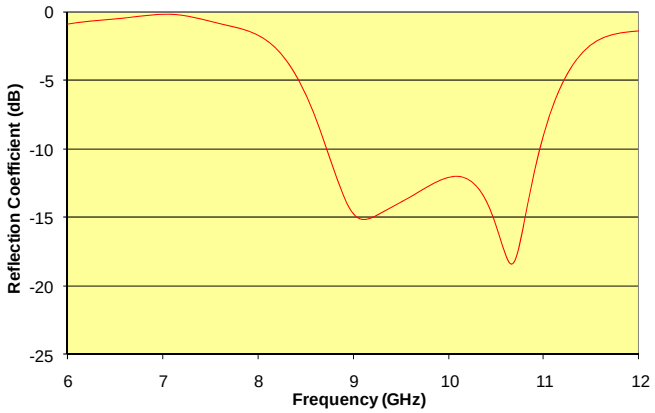

Fig. 4. Predicted reflection coefficient of integrated antenna.

Figure 5 shows the predicted radiation performance of the integrated antenna at 10 GHz. As can be seen from this response, the antenna is efficient and there is some undulation in the response caused by the EOM casing.

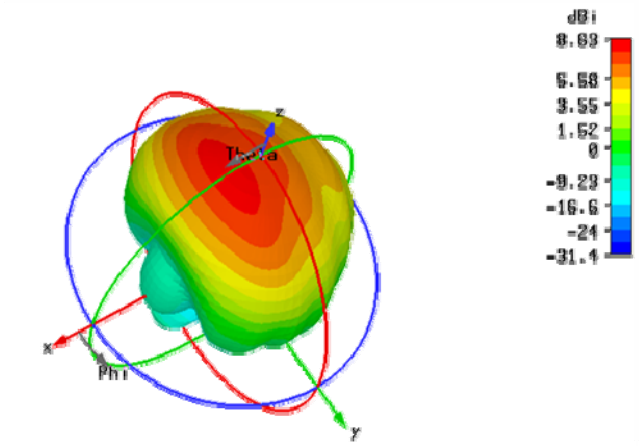

Fig. 5. Predicted radiation performance of integrated antenna at 10 GHz.

III. Proof-of-Concept Version

The predicted results in the previous section were very encouraging. Before we committed to developing the integrated module, we developed a proof-of-concept version of the antenna within the EOM casing assembly to experimentally verify the performance of the antenna. Figure 6 shows a photograph of the developed proof-of-concept antenna. Here we machined the casing out of aluminum and the surrogate feed material is used instead of the $LiNbO_3$ wafer; accordingly the dimensions of the patches were modified to ensure a good impedance match. As can be seen from Figure 6, an SMA connector is used to couple RF power to and from the antenna. Developing this proof-of-concept version enabled us to measure the reflection coefficient and radiation performance of the integrated antenna.

Fig. 6. Photograph of proof-of-concept version of integrated antenna.

Figure 7 shows a comparison of the predicted and measured reflection coefficient of the proof-of-concept integrated antenna. As can be seen from this plot, there is good agreement between theory and experiment.

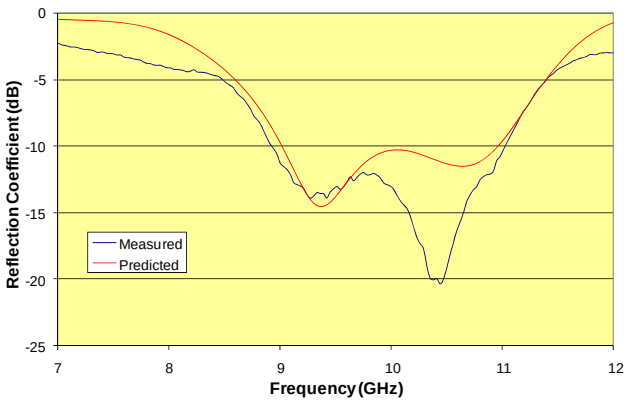

Fig. 7. Reflection coefficient of proof-of-concept version of integrated antenna.

Figure 8 shows the measured co-polar radiation patterns of the integrated antenna at 9.5 GHz. There is some distortion in the radiation patterns, however this is to be expected given the non-symmetric form of the modulator packaging. The measured gain of the antenna in this environment is approximately 8 dBi.

IV. Prototype Results

Figure 9 shows a photograph of the integrated antenna/EOM assembly. The EOM is based on a Z-cut 10 GHz modulator from EOSPACE [3]. As can be seen from this photograph, the antenna resides below the Rexolite cover. The SMA connector allows bias voltage to be applied to the electro-optic modulator.

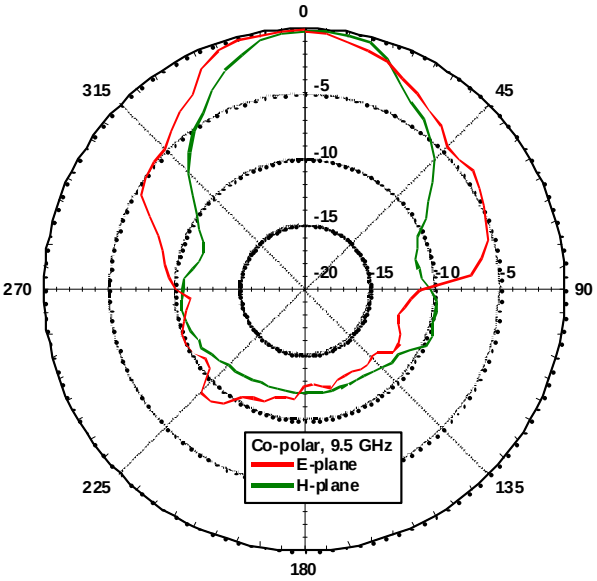

Fig. 8. Measured co-polar radiation patterns of proof-of-concept version of integrated antenna at 9.5 GHz.

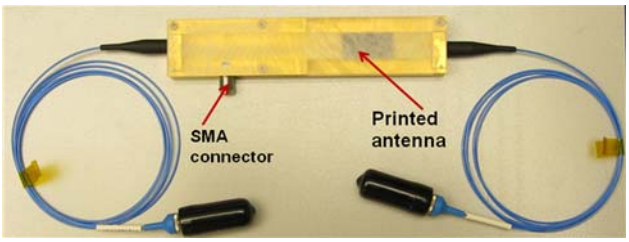

Fig. 9. Photograph of integrated antenna/EOM assembly.

Figure 10 shows the experimental set-up used to measure the transmission properties of the developed integrated antenna/modulator module. The set-up was positioned in our anechoic chamber to ensure minimal multi-path reflections. The source antenna was positioned approximately one meter from the integrated antenna/modulator module.

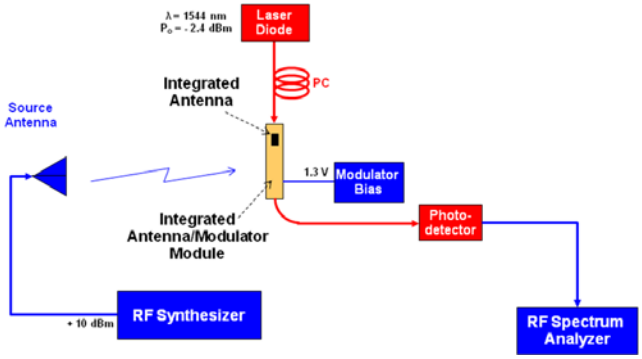

Fig. 10. Experimental set-up to measure transmission performance of the integrated antenna/EOM module.

The transmission response of the integrated antenna/modulator module was measured over a frequency range covering 7 – 12.5 GHz. The link response, normalized with respect to the maximum detected RF power, is shown in Figure 11. The integrated module showed good efficiency over the operational bandwidth of the developed integrated antenna. The maximum received power measured at the spectrum analyzer was -56.9 dBm. A simple link budget analysis was carried out for the measurement set-up shown in Figure 10 taking into consideration the realized gain of the integrated antenna and the characteristics of the modulator as well as other components in the link (photodetector responsivity, transmit optical power, etc). At 9 GHz we estimated that the received RF power at the photodetector terminals, should be approximately -55.8 dBm. These results are in very good agreement with the measured response.

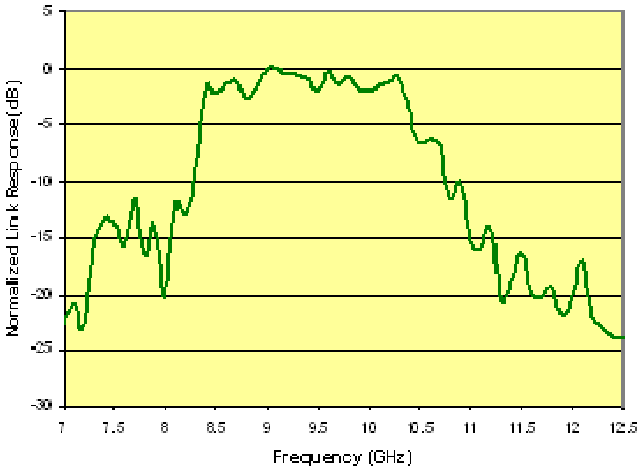

Fig. 11. Measured transmission response of the integrated antenna/EOM assembly.

V. Conclusions

We have discussed the design and development of a novel integrated antenna/EOM module that can be utilized in fiber remoted antenna systems with RF photonic front-ends. The overall configuration and the design philosophy for the integrated module are described. A prototype of the proposed integrated antenna/EOM module was developed and good efficiency over the design band of 9 – 11 GHz was achieved.

References

[1] T. Berceli and P. Herczfeld, "Microwave photonics – A historical perspective *(invited)*," *IEEE Trans. Microwave Theory & Tech.*, vol. 58, no. 11, pp. 2992-3000, November 2010.
[2] W. S. T. Rowe et al, "Investigation into the performance of stacked proximity coupled patches," *IEEE Trans. Ant. & Prop.*, vol. 54, no. 6, pp. 1693 - 1698, June 2006.
[3] http://www.eospace.com/